

Micromachined piconewton force sensor for biophysics investigations

Steven J. Koch,^{a)} Gayle E. Thayer, Alex D. Corwin, and Maarten P. de Boer
Sandia National Laboratories, Albuquerque, New Mexico 87185

(Received 5 June 2006; accepted 2 September 2006; published online 23 October 2006)

We describe a micromachined force sensor that is able to measure forces as small as 1 pN in both air and water. First, we measured the force field produced by an electromagnet on individual 2.8 μm magnetic beads glued to the sensor. By repeating with 11 different beads, we measured a 9% standard deviation in saturation magnetization. We next demonstrated that the sensor was fully functional when immersed in physiological buffer. These results show that the force sensors can be useful for magnetic force calibration and also for measurement of biophysical forces on chip.

© 2006 American Institute of Physics. [DOI: 10.1063/1.2364118]

Functionalized magnetic microspheres are useful for a variety of intracellular and molecular biophysics applications,¹⁻⁴ but their utility depends on the ability to apply well-controlled and calibrated forces. Popular calibration methods have relied on inference of force from the Stokes drag^{3,5} and Brownian dynamics,¹ while other methods have used calibrated microneedles,^{4,6} gravity,⁷ or known properties of polymers.⁸ While very useful, these methods have drawbacks in some cases. In the Stokes drag calibration, the particle radius and solvent viscosity must be known accurately; the magnetic particle may also travel a large distance compared with the particle diameter, leading to complications when the field gradient is large. When using Brownian dynamics, the length of the tether must be measured or deduced, and the temperature must be well controlled. To address these complications, we have designed, fabricated, and tested a compliant surface-micromachined spring with which the lateral force field of an electromagnet on a single magnetic microparticle can be calibrated. This provides a simple force calibration method that does not depend on particle shape, length of polymer tethers, or solvent conditions, and is sensitive enough to allow characterization of a single bead.

As seen in Fig. 1(a), the device consists of gratings attached to a folded-beam suspension, as described in a previous surface micromachining implementation.⁹ It is fabricated by surface micromachining methods¹⁰ using the SUMMiT VTM process, with polycrystalline silicon (polysilicon) as the structural material. The spring constant of the grating can be calculated analytically as

$$k = 2Ew^3t(L_o^3 + L_i^3)^{-1}, \quad (1)$$

where $E=164 \text{ GPa}$ ¹¹ is Young's modulus, $w=0.75 \mu\text{m}$ is the linewidth as measured by high resolution scanning electron microscopy (SEM), $t=2.25 \mu\text{m}$ is the spring thickness, and L_o and L_i are the respective lengths of the outer and inner spring beams, as indicated in Fig. 1(b). For this letter, we use springs with $L_i=542 \mu\text{m}$ and $L_o=561 \mu\text{m}$ having a calculated spring constant of 0.93 pN/nm. To check the accuracy of the calculated spring constant we used NIST traceable mass standard microspheres (Catalog No. 64170, Polysciences) and measured the deflection due to the weight of the microspheres when the chip was turned onto its side.

Using this method (to be described in a forthcoming publication), we obtained a spring constant of $0.76 \pm 0.06 \text{ pN/nm}$. This value is slightly lower than the calculated value, but is reasonable given the strong dependence of the spring constant on the linewidth and the variability in linewidth from chip to chip due to differing linewidth loss across a wafer during processing. Imaging the grating with a numerical aperture of 0.50, 50 \times objective (Olympus LMPlanFI) provides 2.5 nm in-plane displacement resolution and therefore about 1.9 pN force sensitivity. By design, the springs have a maximum deflection of 18 μm , and the deflection remained below 1 μm for all of the data herein. For a 561 μm spring length, a 1 μm deflection is expected to be well within the linear range.

Using two micromanipulators and pulled glass fibers, we affixed with vacuum grease individual beads (DynaM M270 streptavidin, product No. 653.05, lot No. F72000) to a desired location on the microelectromechanical system (MEMS) force sensor with approximately 5 μm precision.¹² Figure 1(c) shows a single bead affixed to a sensor and positioned about 200 μm away from the magnet face. The process required about 10 min/bead and was efficient enough to allow us to individually characterize 11 beads and thus obtain a distribution of saturation moments. To increase efficiency yet minimize uncertainty due to possible linewidth variations, three force sensors fabricated in close proximity were used for these measurements. A control microsphere remained affixed to a fourth sensor throughout all experiments. Figure 2 shows force versus magnet current for 11 different beads at an axial distance of 200 μm from the magnet pole piece. We assumed the saturated bead moment to be proportional to bead displacement at a maximum applied current (20 A, field=660 mT, gradient=21 T/cm, from modeling described below), and constructed the histogram shown in the inset by averaging nine consecutive measurements after stepping currents from 0 to 20 A. For the 11 beads we measured a standard deviation of $\pm 9\%$, compared with less than 1% standard deviation for the control microsphere. The variation is most likely caused by the 3% coefficient of variation in bead diameter reported by the manufacturer. Previous researchers had measured a 72% and 41% standard deviation for a similar magnetic microsphere (DynaM M280).^{5,12} Our much lower standard deviation could reflect improvements in the commercial preparation, or could also reflect uncertainties that arise from the two previous techniques' sensitivity to other factors besides force—

^{a)}Present address: The Center for High Technology Materials, Department of Physics and Astronomy, University of New Mexico, Albuquerque, NM 87106; electronic mail: skoch@chtm.unm.edu

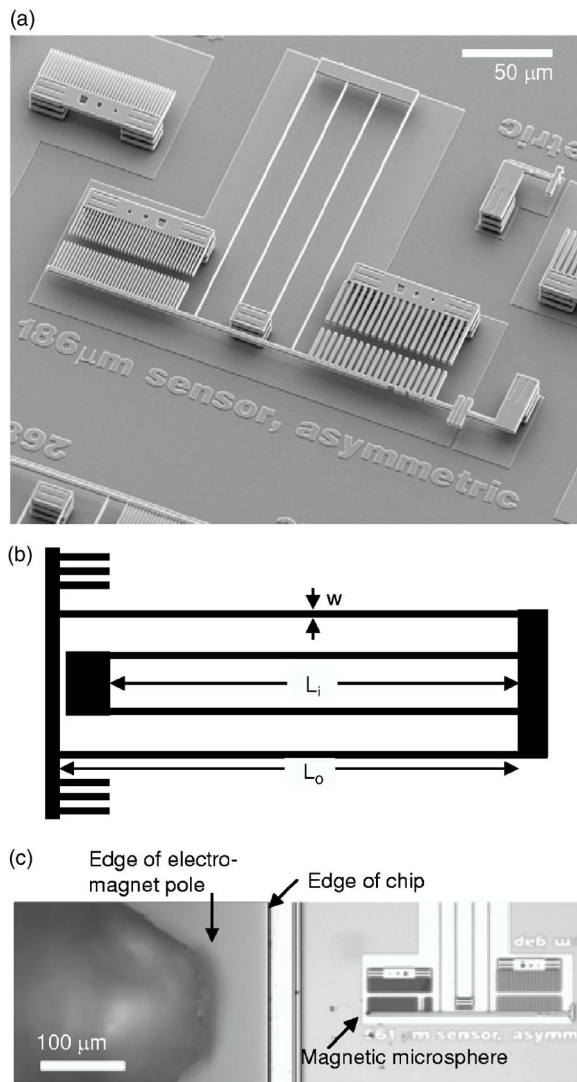


FIG. 1. (a) SEM image of a $L_o=186\ \mu\text{m}$ force transducer ($\sim 30\ \text{pN/nm}$), with a scale bar of $50\ \mu\text{m}$. Stiffer force sensor is shown for ease of display, while a longer, $581\ \mu\text{m}$ force sensor ($\sim 1\ \text{pN/nm}$) is used for data in this report. (b) Schematic illustrating linewidth (w), inner spring length (L_i), and outer spring length (L_o). Not shown is the thickness (t), into the plane of the diagram. (c) $10\times$ picture of the device with single bead positioned near the front face of the electromagnet pole, with a scale bar of $100\ \mu\text{m}$.

namely, bead shape, radius, and viscous coefficient in the former, and orientation and separation of bead from a giant magnetoresistive sensor in the latter. It should also be noted that a potentially high-throughput technique based on a balance between magnetic gradient, gravitational, and Stokes forces has also been reported.¹³ The particles characterized are not directly comparable, and further the technique again relies on many other parameters besides a simple spring constant. We believe that use of a mechanical spring simplifies the bead to bead variation measurement and improves precision.

We also used the microspring to calibrate the force field on a single bead for various currents and axial displacements from the pole, as shown by *open circles* in Fig. 3. For a given distance, the data represent a single current sweep (0 to 10 A, following degaussing), and the same bead and sensor were used for all data. Also shown are axisymmetric finite element magnetic modeling¹⁴ (FEMM) force predictions (*solid lines*) using the manufacturer's specifications of a $2.8\ \mu\text{m}$ diameter and 4.8% volume loading of maghemite

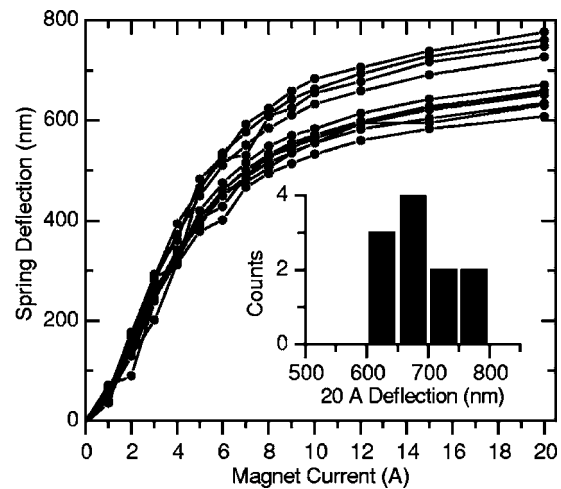


FIG. 2. Measured spring deflection vs magnet current for 11 different beads on three different sensors. Each trace represents an individual nonaveraged sweep with current increasing from 0 to 20 A. Magnet degaussed prior to each sweep. (Inset) Histogram of spring deflection at 20 A; bin size $50\ \text{nm}$. Each measurement represents an average displacement from nine successive image frames (to reduce noise from stray air currents).

nanocrystals with an effective initial susceptibility of 21 and saturation magnetization per unit volume of $417\ 000\ \text{A/m}$. The magnet was modeled with 228 turns of pure copper wire wound around a $3/8\ \text{in.}$ diameter pure iron core. A conical pole piece with an included angle of 64° and a blunt tip diameter of $2.75\ \text{mil}$ was separated from a blunt pole piece by $0.48\ \text{in.}$ Accuracy of the FEMM predictions of the magnetic field and gradient were roughly confirmed using a three-axis hall probe (SENTRON model 3M12-2-2-T). Figure 3 shows reasonable agreement between the measured and modeled forces, but a better fit (not shown) was obtained using a simplex optimization algorithm to fit the effective initial susceptibility and saturation volume magnetization of the maghemite nanocrystals. The best fit value of $494\ 000\ \text{A/m}$ for saturation magnetization was reasonably close to the manufacturer's estimate, but the best fit susceptibility of 2.5 was significantly different from the manufacturer's estimate of 21. Part of this discrepancy can be explained because our measurements are of an isolated microsphere, while the manufacturer's measurements are of

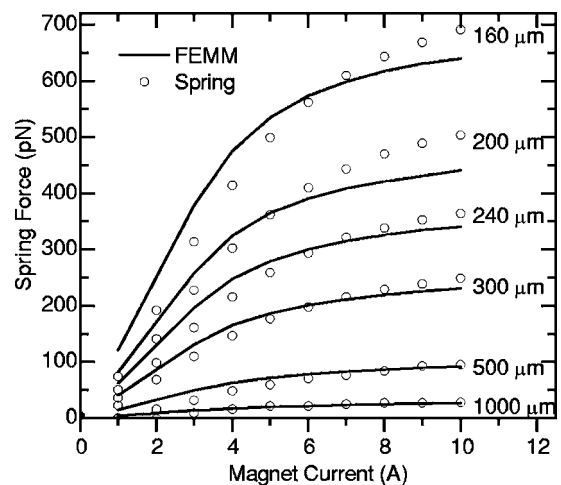


FIG. 3. Measured (open circles) and calculated (lines) force vs applied magnet current for seven different axial displacements of a single bead (from top: $160, 200, 240, 300, 500,$ and $1000\ \mu\text{m}$).

a dried powder, thus incorporating dipole-dipole interactions, but we are unable to explain the approximately eight-fold discrepancy in initial susceptibility. Nevertheless, the similarity of the shapes of the measured and calculated force curves across a wide range of currents and axial displacements lends confidence to the measurement technique. Furthermore, the great difficulty in obtaining reliable magnetic properties of the beads and the large number of estimates and independent measurements that must be incorporated into the modeling technique further illustrate the value of the microspring method as a simple and robust method for calibrating a magnet/microsphere system for use in biophysical applications.

Another feature of the spring force transducer is its relative insensitivity to environmental conditions such as temperature and solvent. We rendered the surface of a new force sensor hydrophilic with an ozone treatment. Then, using a simple flow cell, we hydrated the device and demonstrated full retention of functionality and observed that noise was significantly damped compared with operation in air. While it was not necessary to hydrate the device for magnetic bead characterization, we envision a class of experiments where it will be useful to obtain *in situ* force measurements using the mechanical spring. To demonstrate the viability of this line of experiments, we found that the standard kinesin/microtubule (MT) inverted motility assay was functional on the MEMS device (we saw a similar velocity as seen at room temperature on glass). The current device design was not suitable for measuring forces from the molecular motors. Our next goal is to optimize the sensor geometry to guide molecular motors and to measure, for example, the stall force of a MT shuttle driven by multiple motors, without need for attaching microspheres or other handles. *In situ* force sensing would also obviate the needs to calibrate the electromagnet and magnetic bead and to know the precise location of the bead relative to the magnet pole.

In conclusion, we have shown that a simple micromachined force sensor can be used to characterize individual micron-scale magnetic particles and also to map the magnetic force field of an electromagnet. The principle of our device is similar to previous reports using pulled glass cantilevers^{4,6} and a recent report of a nanomechanical force gauge,¹⁵ but the micromachined spring stiffness is easier to control by design. In the current implementation, the spring constant is best determined via gravitational force on a calibrated mass standard, but future designs will incorporate on-chip electrostatic self-calibration which is not available for glass fibers. Self-calibration combined with the insensitivity to temperature and buffer conditions make the force sensor an attractive alternative to standard magnetic bead calibra-

tion techniques. We anticipate using the device for characterization of other commercial and custom microsphere preparations and other electromagnet designs. Furthermore, we anticipate incorporating the force sensor into future MEMS designs which will be used to measure biophysical forces in real time for a variety of biomolecular and subcellular processes.

We gratefully acknowledge the sample fabrication by the Microelectronics Development Laboratory staff and management at Sandia National Laboratories. We are grateful for SEM by Bonnie McKenzie, for FEM mechanical analysis of sensor design by Frank DelRio, and for access to the micro-manipulator instrumentation in the Materials Characterization Laboratory at Sandia. We thank Jim Martin for help with magnet construction and modeling and George Bachand for helpful technical discussions. Sandia is a multiprogram laboratory operated by Sandia Corporation, a Lockheed Martin Company, for the U.S. Department of Energy's National Nuclear Security Administration under Contract No. DE-AC04-94AL85000.

¹T. R. Strick, J. F. Allemand, D. Bensimon, A. Bensimon, and V. Croquette, *Science* **271**, 1835 (1996).

²F. Ziemann, J. Radler, and E. Sackmann, *Biophys. J.* **66**, 2210 (1994); A. R. Bausch, F. Ziemann, A. A. Boulbitch, K. Jacobson, and E. Sackmann, *ibid.* **75**, 2038 (1998); D. A. Simson, F. Ziemann, M. Strigl, and R. Merkel, *ibid.* **74**, 2080 (1998).

³S. B. Smith, L. Finzi, and C. Bustamante, *Science* **258**, 1122 (1992); C. Danilowicz, V. W. Coljee, C. Bouzigues, D. K. Lubensky, D. R. Nelson, and M. Prentiss, *Proc. Natl. Acad. Sci. U.S.A.* **100**, 1694 (2003).

⁴Anthony H. B. de Vries, Bea E. Krenn, Roel van Driel, and Johannes S. Kanger, *Biophys. J.* **88**, 2137 (2005).

⁵F. Amblard, B. Yurke, A. Pargellis, and S. Leibler, *Rev. Sci. Instrum.* **67**, 818 (1996).

⁶Jie Yan, Dunja Skoko, and John F. Marko, *Phys. Rev. E* **70**, 011905 (2004).

⁷C. H. Chiou and G. B. Lee, *J. Micromech. Microeng.* **15**, 109 (2005).

⁸R. Amit, O. Gileadi, and J. Stavans, *Proc. Natl. Acad. Sci. U.S.A.* **101**, 11605 (2004).

⁹W. C. Tang, T. C. H. Nguyen, and R. T. Howe, *Sens. Actuators* **20**, 25 (1989).

¹⁰J. J. Sniegowski and M. P. de Boer, *Annu. Rev. Mater. Sci.* **30**, 299 (2000).

¹¹B. D. Jensen, M. P. de Boer, N. D. Masters, F. Bitsie, and D. A. LaVan, *J. Microelectromech. Syst.* **10**, 336 (2001).

¹²D. R. Baselt, G. U. Lee, M. Natesan, S. W. Metzger, P. E. Sheehan, and R. J. Colton, *Biosens. Bioelectron.* **13**, 731 (1998).

¹³S. Reddy, L. R. Moore, L. P. Sun, M. Zborowski, and J. J. Chalmers, *Chem. Eng. Sci.* **51**, 947 (1996).

¹⁴D. C. Meeker, *Finite Element Method Magnetics (FEMM)*, Version 3.4.2, 2005, <http://femm.foster-miller.net>.

¹⁵Ki-Hun Jeong, Chris G. Keller, and Luke P. Lee, *Appl. Phys. Lett.* **86**, 193901 (2005).